Hybrid hand: Increasing prosthetic comfort

Design and evaluation of a mechanically supporting hand prosthesis

Ilze van den Brink (4590716), Cilia Claij (4596633), Lisanne van Ooijen (4530853),
Frédérique Oosterbaan (4458613), Hanna Sickler (4552849)

Abstract - At the moment 56% of patients suffering from an amputation wear their hand prosthesis never or once in a while [4]. Prostheses are often difficult in operation, uncomfortable and have an unnatural appearance. The goal of this study is to design a hybrid hand, which will be powered by the muscle strength of a patient and assisted by a motor. A design was excogitated; it was first assembled as test setup and later on put together into a realistic hand prosthesis. The ratio between the forces in the cables and the pinch force were measured without the support of the motor. In addition several tests were executed with the assistance of the motor; the input cable force, maximum pinch force, maximum lifted weight, closing time and weight of the prosthesis were measured. The force needed to be executed by the patient is lower then with a classic hand prosthesis, but the pinch forces are lower then expected due to the fact that the motor driver can not handle that much current. The goal and all but one requirements are achieved, however the design can still be improved by creating a stronger pinch force.

I. Introduction

In the Netherlands about 2400 people have had an upper limb amputation due to trauma or illness and 1350 people are missing a part of their upper limb due to a congenital defect [3]. This is often a traumatic experience that is difficult to process, both mentally and physically. Apart from losing a functioning body part, the appearance of a missing limb attracts unwanted attention. A solution for these predicaments could be the use of a hand prosthesis. Although the use of a prosthesis could help patients suffering from an amputation, the problem is that 56% of them never wear their hand prosthesis due to the fact that they are difficult to operate, uncomfortable and have an unnatural appearance [4] [9].

A distinction can be made between three different types of prostheses; a cosmetic, a body-powered and a myoelectric prosthesis. The cosmetic prosthesis can look extremely natural, but can be expensive and function is sacrificed in order to have a more realistic appearance. The body-powered prostheses are operated by the muscle strength of a patient, but they can be hard to control, have a high operation force and often do not meet the cosmetic standard [9]. The myoelectric prostheses are not powered by the muscle strength, but rather by the electromyographic signals measured on the skin. These signals then control a battery-powered motor to open/close the hand. This last type of prosthesis is quite expensive and prone to errors. Because neither of these types solve the problem of non-wear, an ameliorated prosthesis is needed that improves the desire to actually wear the hand. Combining the strengths of the different types, results in a hybrid hand.

The goal of this project is to design such a hybrid hand, which will be powered by the muscle strength of a patient and assisted by a motor.

This can be achieved by measuring the pulling force on a shoulder cable with sensors and use this measurement to regulate the motor with a microcontroller. Due to the assistance of the motor, the activation power needed to grasp an object will be lower than with a body-powered prosthesis, which will improve the comfort. This is a desired improvement since, in most cases, the muscle strength in the arm decreases after an amputation.

To design and build the hybrid hand, the following design question is formulated: "How can a patient, without a hand, control and regulate the gripping motion of a hand prosthesis using muscle strength and a supporting motor?"

This design question will be elaborated in this paper. In the second chapter, the conceptual phase will be discussed. In chapter three, the design of the hybrid-hand will be developed in subsections for each subsystem. The method used for the testing will be discussed in chapter four, followed by the results in the fifth chapter. Finally, in chapter six there will be a discussion and in the last chapter a conclusion. All the additional information will be provided in the appendices. This design study is part of the Bachelor End Project for Mechanical Engineering students at the Technical University Delft in the third year of the Bachelor studies.

II. Conceptual phase

Based on the different steps of a design process, the design for the mechanical hybrid hand prosthesis was created. This process started with a literature research on existing designs and the way they operate. Based on this literature study, the list of requirements have been set up. Thereafter, the design of the prosthesis was divided into subsystems of which a morphological overview has been composed. At the end of this chapter a concept design will be presented, which will be further elaborated in chapter III.

A. List of requirements

The working mechanism will essentially be composed of the following parts: a shoulder band, mechanics, a motor with transmission, a battery, electronics, the hand itself and the glove to fit over the hand. In section III, the entire working mechanism is described in detail. All parts together will result in a compact hand prosthesis that must meet the following requirements:
The prosthesis has to ...

- ... be operated by a shoulder band (mechanical)
- ... be supported by a motor (electrical)
- ... fit in a glove, standard size 7.5 [7]
- ... be lightweight, not more than 700g
- ... be easy to control
- ... be a working mechanism
- ... output a maximum gripping force of 35N

B. Morphological analysis

During the design process different concepts were created, each with their own strengths and weaknesses. To analyze the various ideas, subsystems were made to find partial solutions. The solutions were compared in a morphological analysis, which can be found in appendix A. In this section, solutions for three subsystems will be discussed.

A concept had to be developed to connect the fingers to the cable. One idea is based on a trash grabber (figure 1), containing a rotating disk attached to the cable and fingers. A disadvantage of this system is that it is not resistant to dirt, like sand that would come through small gaps of the outer shell, as it can easily be blocked. Moreover, the system would only enable the thumb or fingers to move instead of both of them. In another concept, multiple gearwheels are used to enable the transmission between the cable and the fingers, this would allow the fingers and thumb to work simultaneously. However, as stated above, this will not function for prosthesis used on a daily basis due to dirt that could cause the gearwheels to wear out, when the hand would

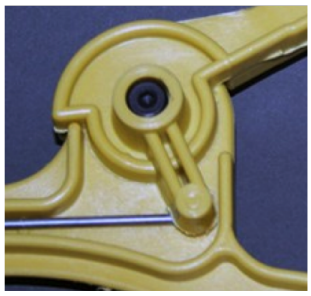

Fig. 1: Mechanism for opening and closing a trash grabber.

be used in daily life. In addition to these designs there are also concepts based on pulleys, chains, a lever and rack and pinion, these are shown in appendix A. Eventually, a solution was found in a prosthesis designed by Riho Markna, for his master's thesis at the department of BioMechanical Engineering (BME), Delft University of Technology [8]. He used a simple, practical and robust design using a bar linkage which tested to even work with sand between the rods. From the concept phase it can be concluded that the linkage system is the preferred connection, due to its simplicity and durability.

For the remaining subsystems, several ideas have been developed. The first subsystem is the transmission from the motor to the cable (including a transmission ratio). The second subsystem is the operating system of blocking the fingers when they are closed to enable the motor to stop turning, otherwise the motor has to deliver too much power and will get hot.

For the first subsystem pulleys, planetary gears, a rack and pinion gear and a worm and worm gear have been investigated. The motor has a rotating output, this could be used to directly drive planetary gears or pulleys, which close the fingers or roll up the cable attached to the fingers along an axis. The rotating output of the motor could also be used to drive the pinion gear. The rack could be used to execute a translational motion of the cable. The problem with these solutions is that the motor needs to have a 90° angle with respect to the cable, but very limited space is available in the hand prosthesis to implement this. The solution of using a worm and worm gear has the advantage that the motor can be placed in line with the cable, as there is a 90° angle present in this construction. There is more space available to place it this way.

Solutions for the second subsystem were a ratchet and a worm and worm gear. These systems can only be driven by the motor in one direction and

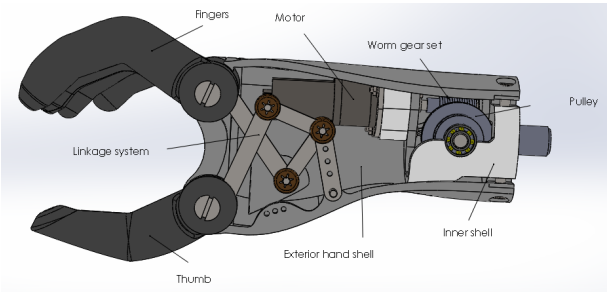

Fig. 2: Overview of the current design in SolidWorks.

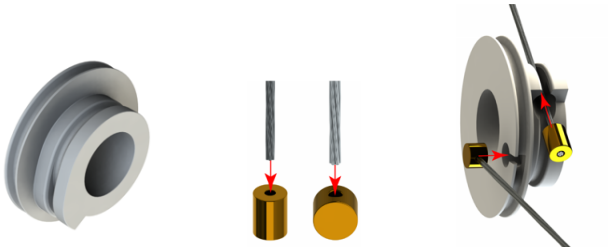

(a) A 3D model of the pulley.

(b) Bushings are soldered for the cable attachment.

(c) Easy assembly.

Fig. 3: Changing the travel distance is achieved by the wheel and axle principle. The input and the output cables are sitting on different radii [8].

when the motor stops turning, they prevent motion in the opposite direction, caused by potential forces on the cable. The main disadvantage of the ratchet is that the motor can not be placed in line with the cable. Hence, the worm and worm gear were also the best solution for this subsystem.

From this section, it becomes clear that several subsystems are in line with the hand Riho designed. In the hand Riho designed, an inner shell is present to mount the motor, worm and worm gear. Because of this shell, the worm and worm gear are protected from dirt. The previously stated argument against gears does not apply inside the inner shell, thus the worm and worm gear can be used.

III. Detailed design

As explained in section II-B, this design and the the design of Riho are the same in several aspects. That is why the decision was made to improve the prosthesis Riho designed, instead of designing a whole prosthesis from scratch. In this section, the adjustments made to the design of Riho will be discussed.

A. Detailed design analysis

In this section a detailed design analysis of the hybrid hand is presented. To understand where the components will be located and what their function is, an overview of the SolidWorks model can be seen in figure 2 (this figure is presented again in appendix B on a larger scale). The application of these components is further elaborated in sections III-A1 to III-A8. Appendix B shows three assembly drawings of the hybrid hand. An overview of all components used in the hybrid hand can be seen in appendix C.

The mechanism for closing the hand is based on the following operating system: two cables are attached to the double pulley inside the inner shell. The cable on the outer radius is attached to the shoulder cable. As soon as the shoulder cable is pulled, this cable will turn the pulley. Turning the pulley causes the cable over the inner radius to roll around the pulley. This cable is attached to the linkage mechanism, which results in a translational motion. The thumb and fingers come together, closing the hand. The motor and worm gearset support the mechanism by rotating the axis of the pulley.

1) Linkage system and fingers: The linkage system did not contain any defects so this design is used. The rods are made of stainless steel and have been made using laser cutting. To ensure a secure fixation, without loosing the ability to rotate, pins were used enclosed by starlocks. Three out of four pins are 2mm, because they are easier available than 3mm pins. For the last pin the decision has been made to keep the 3mm one, due to the fact that the guidelink endures a greater force than the rest of the links. Furthermore the fingers of the hand were made by 3D-printing, using a ultimaker printer provided by the Technical University of Delft

2) Pulley and tensioning shoulder cable: The pulley had been changed by mirroring it. It is fabricated using 3D printing and has two different radii as can be found in figure 3. The cable that is connected to the shoulder cable rolls around the large radius ($r_{large} = 13.7\,mm$). The radius of this part of the pulley is the maximum radius possible to fit in the inner shell. The cable that is connected to the linkage system, rolls over the part with the smaller diameter ($r_{small} = 9.1\,mm$). This diameter is determined by the horizontal displacement the linkage system has to execute in order to close the hand [8]. The cables are attached to the pulley by two small brass bushings. To attach the bushings to the cable hard soldering has been used. Flux 1802 N is used to let the solder flow through the bushings and to avoid oxidation.

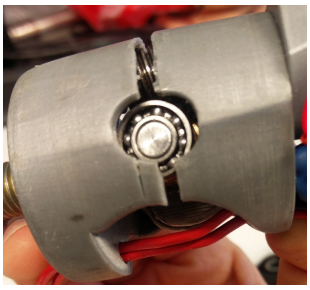

Fig. 4: Due to faulty orientation of printing and the forces exerted on the housing, an earlier design broke. Here, the fault line can be seen [11].

The pulley is fixed on a roller clutch, therefore the pulley can move freely around the axis. This allows the hand to close with only body power. As soon as the motor starts to help, the pulley will still turn in the correct direction.

The mirroring of the pulley has been necessary due to a defect of the motor axis. The axis has a deviation because it was self-made. To minimize the swerve of the axis, the worm had to be reversed. Unfortunately, it was already glued to the axis. To eventually solve the issue, the roller clutch had to be reversed and as a result the motor needed to run the other way around. This causes a new complication namely the brass bushing on the small radius was not locked by shape anymore, meaning it will be pulled out of its socket. This issue was resolved by mirroring the pulley.

Furthermore, a problem with the original design is that the part of the cable that is connected to the shoulder cable would fall off the pulley when the hand is returned back to the opened position. The cable would fall off the pulley due to the lack of tension at this point. This problem is caused by the fact that the pulley turns along with the motor axis. As soon as the patient returns his/her arm to the resting position there will be an exceeding amount of cable causing it to fall off the pulley. The solution is to mount a spring just outside the hand shell to keep the cable in tension at all times.

3) Inner shell: An inner shell keeps the motor, worm, worm wheel, pulley and clutch in place. During previous tests that Riho executed, this shell broke apart due to forces exerted by the worm wheel. This part is adjusted by printing the part with a 90° orientation with respect to the fault line (see figure 4). The structural design of the part also has been modified, small connections have been made bigger, this can be seen in appendix B.

4) Motor and worm gear set: The worm and worm wheel that were used initially are not easily obtainable, that is why a different set was chosen. In this design, a worm with a single start is used, meaning for each 360° turn of the worm, the worm-wheel advances only one tooth of the gear wheel. The corresponding worm wheel has 20 teeth, this gives a transmission ratio of 20:1 (*startsworm* : *teethwormwheel*). The motor has to exert a minimum force of 75 N to result in a minimum pinch force of 15 N between the fingers and thumb [8]. The minimum motor force results in a minimum torque of $\approx$ 1.1 Nm at the pulley axis as can be seen in equation 1. So by choosing another worm and worm wheel, a different motor had to be selected as well in order to still obtain the minimum torque. A brushed motor from Pololu, including a gearbox with a ratio of 25:1, and a stall torque of $\approx$ 0.155 Nm at the outgoing axis was picked. A brushed motor was chosen because brushless motors need more and more complex wiring, meaning the designer has to have a decent amount of knowledge about electronics. Using this motor results in a total system transmission of 500:1 and a torque of $\approx 2.48\,Nm$ at the pulley axis. This torque can be calculated with equation 2. The total system efficiency (from motor via worm and worm gear to pulley) has been estimated at 0.8 [8].

$$F_{motor,min} \cdot r_{pulley,in} = 75\,N \cdot 13.7\,mm \tag{1}$$

$$\begin{aligned} T_{pulley} &= T_{motor} \cdot i \cdot \eta_{system} \\ T_{pulley} &= 0.155\,Nm \cdot 20 \cdot 0.8 \approx 2.48\,Nm \end{aligned} \tag{2}$$

By choosing a new worm, worm wheel and motor, some dimensions were changed as well. To assemble these components, two new axes were designed on which the worm, worm gear, clutch and pulley were installed. The axes are mounted with SKF 618/4 (2x), SKF 618/5 and SKF 618/6 bearings in the inner shell.

The motor axis is attached to the axis with the worm by using two motor clamps. The axis with the worm has a gap that fits the motor axis. The clamps ensure that the axes both rotate. This system is protected by a 3D printed motor shell. In appendix B an overview of this mounting mechanism is presented.

5) Exterior hand shell: The hand shell contained a few flaws. The linkage system scraped against the inside surface of the hand shell (see figure 5). This problem is solved by making the recess at this point bigger and also making the outside of the shell thicker to avoid a hole in the shell. Moreover, the holes created for the spring-holding pin are too close to the edge. The small fringe of 3D printed material is not strong enough to hold the forces

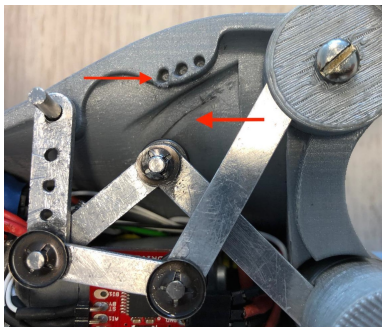

Fig. 5: The outer shell of the previous design lacked material around the mount for the spring, this caused it to deform. At a different location the linkage system scraped the exterior.

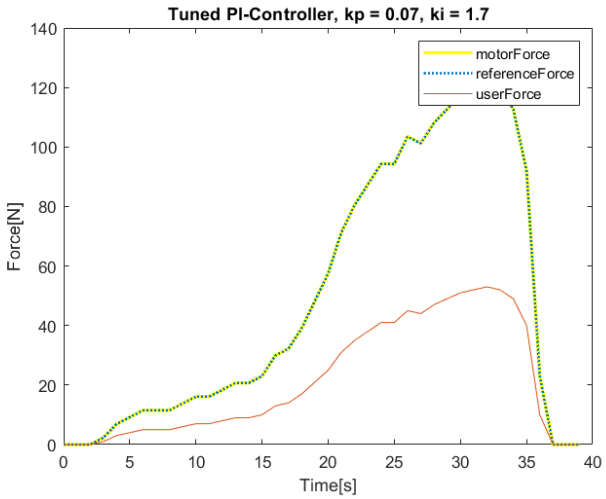

Fig. 6: The motorForce and referenceForce are perfectly alligned, which means the PI-controller is tuned correctly.

of the spring, which causes it to deform as can be seen in figure 5. To solve this problem the holes are relocated 0,75 mm, creating a larger edge and thus a stronger grip for the spring.

6) Electronics: Different electronic components are used in the design and these different components will be discussed in this subsection.

For easy speed and motion control, a motor controller is used. Two controllers were ordered. The first one is small and fits in the hand, but can handle a constant current of 1.2 A and a peak of 3.2 A for 10 ms, while the stall current of the motor is 2.9 A. The second controller can handle a constant current of 2 A, but is too big to fit in the hand.

Two force sensors from Futek are used to measure various forces that are necessary. They are used to control the motor. The first sensor is placed between the cable connected to the pulley and the shoulder cable, this sensor can measure up to approximately 100 N. The second sensor is placed between the linkage mechanism and the cable mounted to the pulley, this sensor has a maximum of approximately 300 N. An overview of all sensors, including one that is used for testing, can be found in figure 7.

In order to correctly read out the values of the sensors, INA125P amplifiers of Texas Instruments are necessary. The output voltage of the Futek sensors is 2.5 mV - 10 mV, when they are powered with 5 V. The amplifiers are used to map this range to 0-5 V, which makes it possible to read the sensor values with the Arduino. These specific amplifiers are chosen because they are small, cheap, simple to use and fit the purpose for the used sensors. The amplifiers are soldered to a printed circuit board, and connected to the Arduino with electrical wires.

To process the measured forces and control the motors, a microcontroller has been used. The Joy-it Arduino Nano V3 is used due to size, prize and functionality compared to similar microcontrollers.

7) Code: The existing code [8] worked sufficiently with his model. However, the code includes some non basic programming elements, which took some time to understand. After testing with the new design, and thus new components, the code did not work well. Some variables used by in this existing code needed to be changed, because of the new components. These changes could not be made easily, because the purpose of some variables was not clear. Therefore the decision has been made to write a new code. The main goal of the code is to control the motor, using the measured forces. To prevent random peaks in the userforce from interfering with the system, the forces are averaged over ten measurements. The mean userforce value is compared to a reference value and the error between the two is used in a PI-controller. This controller has been tuned using MATLAB R2018b. Because a PI-controller gives significantly better results than a PID- or PD-controller, the decision has been made to only use a PI-controller. As can be seen in figure 6, the motorforce perfectly follows the referenceforce while using the PI-controller. The data used to calculate the userforce is real data obtained during testing.

To calculate the reference force, it is needed to estimate the performance of the hand. The best way this can be done, is to look at the performance of the hand of Riho. The maximum gripping force

he measured was approximately 35 N [8]. The maximum force a user can apply strongly depends on the person. Because of that, it is difficult to estimate the maximum user force. However the research of Monod H. shows a mean userforce of 38 $\pm$ 17 N for women and 66 $\pm$ 23 N for men with the shoulder cable motion [10]. Without restricting certain people from using the hand, an input force of 35 N has been used. This value needs to be changed and adjusted to the user when testing the hand. Using the maximum gripping force and input force (this ratio is 1), the reference force can be calculated with equation 3. The values 1.3 and 3.6 respectively are the ratios inBetweenForce:userForce and inbetweenForce:grippingForce. These ratios are determined during the first tests with the test setup. The userForce, and thus the inBetweenForce, can have peaks which can interfere with the data. To prevent this, the mean value of ten measurements is used. Because ten values need to be saved during different loops, a special package to use circularBuffers is imported. These buffers save ten values and overwrite the oldest value when there is no space to save an extra value. The motor is turned on until the desired gripping force is reached. To open the hand, the userForce has to decrease by 2.5 N, to prevent the hand from opening too early.

$$\begin{aligned} \frac{userForce*1.3+referenceForce}{3.6} &= grippingForce \\ userForce*1.3+referenceForce &= userForce*3.6 \\ referenceForce &= userForce*2.3 \end{aligned} \tag{3}$$

8) Ball receiver and bolt: In order to secure the hand prosthesis, a large bolt is used that is mounted to the inner shell. Furthermore, a ball receiver is necessary. This is the connection between the shoulder cable and the cable inside the prosthesis. The old design did not meet the requirements, because the ball connected to the shoulder cable was not fixed in the connection. So without cable tension the ball could leave the cube and the connection would be lost. A new design has been made in which the ball is kept in place independent of the cable tension (see appendix B for the SolidWorks design). The newly designed cube is always closed on one side and the other side can be closed with a small plate. This prevents the ball from leaving the cube at both sides. The shoulder cable exists the cube from the top and the cable from the hand can be mounted at the bottom.

IV. Method

In this section the test setup will be explained in detail. Except from that it is also discussed in which way all the tests will be executed. Finally, an indication of the expected results will be given.

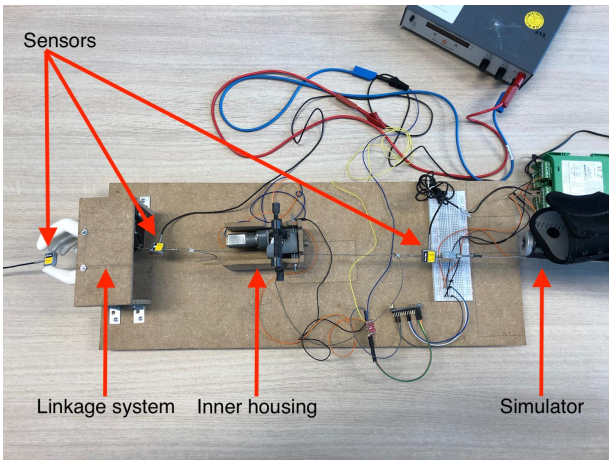

Fig. 7: Overview of the complete test setup from above. The different sensors and subsystems of the system are indicated in the figure.

A. Test setup

The test setup was built on a wooden plate, instead of testing the system directly in the hand in order to elongate the system, as can be seen in figure 7. This makes it easier to adjust the setup when an error arises. The wooden base is strengthened with a second plate to reduce bending.

The linkage system and the fingers are mounted in a similar way as they would be in the hand prosthesis. To reduce the rotation of the axis through the fingers, one plate is mounted on top and two plates are mounted on the side fastened by four angular metal plates (figure 7). In the final design the linkage system is attached to the handshell, to mimic this connection an adjustable stainless steel plate is used as can be seen in figure 8. This will secure the guidelink and the spring while testing.

The inner shell is mounted to a wooden U-shape by rifling. The motor is supported by a wooden cube to reduce a moment force. This can be seen in the overview of the test setup in figure 7.

A third force sensor is placed between the fingers to measure the pinch force. This sensor is calibrated at 40 N since the desired gripping force is 35 N. Because it is calibrated in tension and the sensor itself will be loaded in compression, the measured values will be negative. The exact placement of the three sensors can be found in figure 7.

B. Test method

To check the operation of the hand prosthesis, the test set-up is used. Several tests were executed,

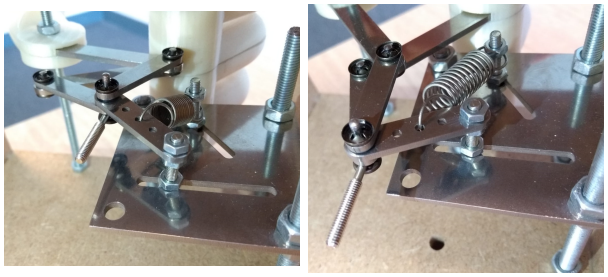

(a) Orientation of the system when the hand is opened.

(b) Orientation of the system when the hand is closed.

Fig. 8: Detailed view of the test setup of the linkage system.

which provide information about the following.

First of all, the forces on the three force sensors are to be measured. These test results are obtained by pulling the cable without using the shoulder cable. The sensor between fingers and thumb is calibrated on tension, but loaded on compression and the sensors between the cables are calibrated and loaded on tension. The computer displays the forces. This test will be executed ten times and gives the average ratio between the forces on the cable and the gripping force without the support of the motor. Second, the motor is set to the maximum power it can deliver with the small motor controller (6 V, 1.2 A). The computer displays the forces. This test will be executed ten times and gives the average gripping force and the average forces on the cable with the support of the motor.

The maximum weight that the prosthesis can carry, is tested by trial and error. Different weights are lifted by the prosthesis with support of the motor until the hand drops them, this can be concluded as the maximum weight. This weight depends on the friction coefficient of the different materials involved.

After using the test setup, it is important to create the real prosthesis, measure its weight and capabilities could be tested. The weight of the prosthesis is measured using a measuring scale. The opening time of the prosthetic hand is tested by measuring time with the high speed camera of a GoPro HERO5. Time measuring starts when the hand starts to close. The test will be executed three times and gives the average.

C. Expected results

The maximum gripping force depends on the force exerted by the user and the motor. Women can operate a body-powered prosthesis fatigue-free up to 38 $\pm$ 17 N, whereas males can handle forces up to 66 $\pm$ 23 N [10]. The motor gives a maximum cable force around 250 N. While using the prosthetic hand the user often does not give the maximum fatigue-free force, during the tests a maximum cable force of 35 N is used. Meaning the pinch force between the fingers and thumb will add up to 35 N when the motor is assisting and around 10 N if it is not. These results may differ depending on the user, a grown man will apply more power than a child.

The maximum weight that the prosthesis can carry depends on the friction coefficients of the two materials involved. Assuming plastic and metal are used the friction coefficient is 0.3, the applied force is between 15 - 20 N and the motor support results in a pinch force of 35 N [2] [5].

The predicted maximum weight that can be lifted by the prosthesis will be 0.460 kg if the hand is body powered and 1.070 kg with assistance of the motor as can be seen in equations 4 and 5, respectively.

$$\begin{aligned} u * F_{normal} &= m * g \\ 0.3 * 15 &= m * 9.81 \\ m &= 0.460kg \end{aligned} \tag{4}$$

$$\begin{aligned} 0.3 * 35 &= m * 9.81 \\ m &= 1.070kg \end{aligned} \tag{5}$$

These results are predicted based on a friction coefficient between metal and plastic. When the prosthesis is being finalized it will be covered with a rubber glove to make it appear more realistic. Rubber has a higher friction coefficient then plastic, so the eventual maximum weight that can be lifted will probably be higher then the expected value.

The motor has a speed of 590 rpm at maximum power, this results in an opening time of approximately 1.18 seconds. This can be calculated with equation 6.

$$\begin{aligned} t_{opening} &= \frac{x_{cable}}{2 \cdot \pi \cdot r_{small}} \cdot \frac{1}{v_{motor}} \cdot 60 \\ t_{opening} &= \frac{33.21\,mm}{57.1769863\,mm} \cdot \frac{1}{590\,rpm} \cdot 60\,s \approx 1.18\,s \end{aligned} \tag{6}$$

The weight of the prosthesis will be heavier than a normal hand which is 0.426 $\pm$ 0.063 kg [6]. The prosthesis is expected to weigh about 500 g.

V. Results

In this section, the test results will be given. Appendix E presents three figures of the complete hybrid hand.

A. Test ratio forces without motor

In figure 9 the results of the first tests are shown. The force on the cable connected to the shoulder cable, the force on the cable between the fingers and the motor and the gripping force are plotted against time.

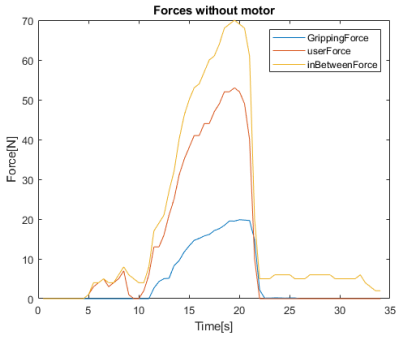

Fig. 9: The forces measured by the different sensors. In this test the cable is pulled without without shoulder band and without motor support.

B. Test ratio forces with motor

In figure 10 the results of the second test are shown. The force on the cable connected to the shoulder cable (orange), the force on the cable between the fingers and the motor (yellow) and the gripping force (blue) are shown. The motor started helping from the moment a force of 15 N was measured at the shoulder cable. At that moment, the user is able to stop delivering a force. The maximum measured gripping force is 10.877 $\pm$ 0.0005 N. The maximum force on the cable between the fingers and the motor is 59.36 $\pm$ 0.005 N.

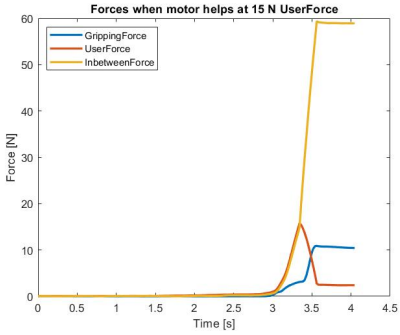

Fig. 10: The forces measured by the different sensors are plotted against time. The motor started to help from the moment the UserForce was 15 N.

C. Test weight

In table I the results of the test with different weights and materials are shown. The material, the weight, the friction coefficient and if the hand clamps the object or not are tabulated. During these tests, the gripping force has not been measured. However, the tension on the cable between the fingers and the pulley has been measured and was on average between 60 N and 66 N.

TABLE I: Test with different materials and weights.

Material	Weight [kg]	Friction coefficient	Clamp yes/no
Adjustable wrench	0.370$\pm$0.0005	0.25-0.4 [2]	Yes
Aluminum block	0.395$\pm$0.0005	0.4 [5]	Yes
Aluminum block	0.715$\pm$0.0005	0.4 [5]	Yes
Steel plate	0.835$\pm$0.0005	0.25-0.4 [2]	No

D. Test opening time

The results of the test of the opening time are presented in this section. This test was done using a high speed camera, GoPro HERO5. The time started when the first movement was observed and ends when the fingers and thumb were fully opened. The average opening time is 1.93 seconds.

E. Prosthesis weight

The weight of the prosthesis is 0.455$\pm$0.005kg without the battery and 0.559$\pm$0.005kg including the battery.

VI. Discussion

In this chapter, the test results and design choices will be discussed. The results will be compared to the expectations and the design will be discussed based on errors during testing. A few recommendations are made for future research on this project of designing a hybrid prosthetic hand.

A. Discussion of the test results

During testing, it became clear that the forces the prosthesis delivers are lower than expected. Without the support of the motor, the maximum gripping force measured is 20 N. With the support of the motor (6 V, 1.2 A), the maximum measured gripping force is 11 N. The maximum force on the cable between the fingers and the pulley with the support of the motor while holding different weights has been measured as 66 N. Due to the lower forces that have been measured,

lower weights than expected could be gripped. Also opening time is effected by the lower forces.

The first reason for this result, is that the bushing mounted in the smaller pulley is to big. This results in the fact that, when testing without the support of the motor, the ratio from the big pulley to the small pulley is about 1, while should have been approximately 1.5. This can be caused by friction inside the inner shell. As a result, the force delivered by the user is not amplified as much as expected.

Another reason is that the motor driver used for the test with the support of the motor is small so it would fit in the hand. This means the motor driver could only resist a current of 3.2 A for 10 ms and a constant current of 1.2 A while the motor has a stall current of 2.9 A. Hence, the motor can not deliver maximum power. It would be recommended to find a small motor driver that can handle the high stall current. A possibility is the TB9051FTG Single Brushed DC Motor Driver Carrier, this motor driver can handle a peak current of 5 A and 2.6 A continuous. There is also a option to investigate brushless motors, they are more common with a broader choice of motor drivers.

The weight of the prosthesis is almost the same as the expected weight. Namely the prosthesis is 0.559$\pm$0.005kg and it was predicted at 0.500$\pm$0.005kg, meaning there is only an error of 0.059kg. Compared to a human hand, which is 0.426 $\pm$ 0.063 kg, it is heavier. However, this difference is negligible.

B. Components outside the hand shell

Unfortunately some components did not fit in the hand because they were too big. These will be discussed in this section.

1) Battery: The battery is had to be installed outside of the hand shell due to the lack of internal space. To fit in the hand and create a more natural look for the prosthesis, a smaller battery is needed. This battery still needs to apply the same voltage of 6V.

2) Amplifier board: The printed circuit board that is used to attach the amplifiers is quite large, namely 100x30 mm. This can be reduced significantly if the amplifiers are positioned closer together or two circuit boards are used and positioned on top of one another.

3) Pulley tensioner: To solve the problem of the cable running off the pulley, a design was made to use a spring to keep the cable in tension. Unfortunately the spring could not be installed inside the hand shell, so it was placed just outside of it in the design. There was no time available anymore to test if the pulley tensioner solves the issue. However, it is not desired to have components exterior of the shell. It is recommended to install the spring inside the hand shell or to find a comprehensively different solution.

C. Other problems

1) 3D-printing: The hybrid hand contains multiple parts that are made with a 3D printer; the fingers, exterior shell, inner shell and pulley. When printing these parts the holes often cause a problem. With 3D printing it is not possible to obtain the exact diameter. To solve this problem, it is recommended to print the holes with a diameter that is approximately 3 mm smaller than needed. The exact diameter can be achieved with the use of a pillar drill if the shape of the part is easy to clasp or drilling out by hand.

2) Ball receiver: The ball receiver does not slide smoothly over the simulator due to the fact that the current design is in the shape of a cube. The corners of the cube get stuck behind the simulator when the shoulder cable is pulled. To solve this problem, the ball receiver in appendix D can be ordered online if there is enough time and budget available. If the right resources are available it could also be possible to copy the design and make it by hand.

3) Scraping inside the exterior hand shell: In the existing model the linkage system scraped over the exterior hand shell. Due to this problem the shell was adjusted. The new design contains a small bulge to locally thicken the surface so the recess for the linkage system could be increased. This bulge will not be visible when the glove is fitted over the prosthesis but in the future it would be preferred to make the transition smoother. This could be done by changing the surface of the shell. Doing so could change the shape of the shell at all sections which could lead to a misfit of the inner shell, so both shells need to be adjusted.

4) Worm gear set: The function of the worm gear set is to establish a transmission from the motor axis to the pulley. The current worm gear set is chosen based on delivery time and budget. This set was easy to obtain and not too expensive. The disadvantage is that both the worm and the worm gear had to be glued on a self-designed and self-made axis. This resulted in alignment problems that could be prevented by ordering a precision shaft worm at Ondrives.

5) Orientation of the shoulder cable: Due to alignment problems with the motor, worm and pulley, the cable leaves the hand prosthesis at the opposite

side with respect to the desired side. This is inconvenient, because the cable will run underneath or over the forearm, possibly causing undesired discomfort. It is possible to let the cable exit the hand on the right side, but then the problem arises that the cable will make a turn of 90° exerting extra forces on the cable and friction on the inner shell. As mentioned in section III-A2, the whole problem started with the self-made axes. When these axes are ordered at Ondrives, this time consuming problem can be prevented.

VII. Conclusion

To conclude, the use of a body-powered hybrid hand prosthesis can be controlled and regulated by a PI-controller that is based on test results. These results are based on tests that have been executed with the hand prosthesis while the motor was off. During these tests, the ratio between the shoulder cable, the cable between the fingers and the motor and the gripping force was determined. With this ratio, the power that the motor has to deliver was determined to support the gripping motion sufficiently. The motor starts assisting when force of 15 N is measured in the shoulder cable. This signal is sent back to the microcontroller (Arduino) to switch on the motor.

The design of the hand prosthesis is based on the design from the master thesis of Riho Markna. A lot of convenient improvements have been made to the prosthesis during this final project, creating a superior design to the one before. The inner shell is stronger and will not break while using the prosthesis, the exterior hand shell is adjusted so that the linkage system does not scratch the surface resulting in a smoother motion. The code used to direct the hand prosthesis is simplified, making it easier to adjust and easier to understand for future designers. Furthermore, a new design for the ball receiver has been made, making it impossible for the shoulder cable to fall off. Last but not least, adjustments were made concerning the pulley, first of all it was mirrored and secondly the problem with the cable rolling off was resolved by adding a spring to keep the tension in the cable.

The goal of this study was to design a hybrid hand, which will be powered by the muscle strength of a patient and assisted by a motor. This goal is achieved and on top of that all but on of the requirements are met. Meaning it is operated by a shoulder band, supported by a motor, it fits in a glove, it is lightweight, easy to control, and it is fully operational. The only requirement that is not met is the gripping force of 35N due to the fact that the motor driver could not handle that much current. Although the prosthesis is sufficiently upgraded compared to its predecessor, there is still room for improvements such as modifications to the motor driver, worm axis and ball receiver.

Acknowledgements

We would like to thank Dr.ir. G. Smit for offering us this challenging, complex and educational bachelor final project. In addition we would like to thank him for the support and critical advise during our project. Furthermore, we would like to thank Ing. J. van Frankenhuyzen for helping us during our design phase and advising us on the different possibilities of our project. Finally, we would like to thank J. van Driel, W. Velt, J. Gijzemijter and R. van Antwerpen for assisting us during testing and manufacturing.

References

[1] Ball receivers [Digital image]. (n.d.). Retrieved June 4, 2019, from https://www.spsco.com/by-product-type/prosthetics/upper-extremity/harness-parts.html

[2] Coefficient of friction for a range of material combinations. (n.d.). Retrieved June 6, 2019, from http://www.tribology-abc.com/abc/cof.htm

[3] Dijk AJ van. (2007). Terminologie, classificatie, registratie en epidemiologie van defecten aan de bovenste extremiteit. In:Brouwers MAH, Mulders A, editors. Amputatie en Prothesiologie van de bovenste extremiteit. Nijmegen: Bureau PAOG-Heyendael; p. 10–35.

[4] Davidson, J. (2002). A survey of the satisfaction of upper limb amputees with their prostheses, their lifestyles, and their abilities. Journal of Hand Therapy, 15(1), pp.62-70.

[5] Elert, G. (n.d.). Coefficients of Friction for Aluminum. Retrieved June 6, 2019, from https://hypertextbook.com/facts/2005/aluminum.shtml

[6] G. A. Kragten, J. L. Herder, and F. C. T. v d Helm, "Design guidelines for a large grasp range in underactuated hands," 2010.

[7] G. Smit, R. M. Bongers, C. K. Sluis, and D. H. Plettenburg, "Efficiency of voluntary opening hand and hook prosthetic devices, 24 years of develop- ment?" Journal of Rehabilitation Research and Development, vol. 49, pp. 523–534, 2012.

[8] Markna, R. (2018). SIMPLE UPPER LIMB PROSTHESIS WITH EXTERNAL POWER SUPPORT FOR CINEPLASTIC CONTROL (Unpublished master's thesis). Delft University of Technology. Retrieved April/May, 2019, from http://resolver.tudelft.nl/uuid:00c21737-a4f8-4df8-b582-f5c758e4d323

[9] Micera, S., Carpaneto, J., & Raspopovic, S. (2010). Control of Hand Prostheses Using Peripheral Information. IEEE Reviews in Biomedical Engineering, 3, 48-68. doi:10.1109/rbme.2010.2085429 https://ieeexplore-ieee-org.tudelft.idm.oclc.org/stamp/stamp.jsp?tp=arnumber=5598519

[10] Monod H. Contractility of muscle during prolonged static and repetitive dynamic activity. Ergonomics. 1985;28(1):81–9.

[11] Popescu-Tamas, L. (n.d.). Technical documentation for the Hybrid Hand Prosthesis [PDF].

A Morphological analysis

This appendix presents the design ideas that are conceived as possible applications for a mechanical hybrid hand. Table 1 shows the design ideas for each submechanism. Figure A.1 to A.4 show four interesting drawings of the design ideas.

Table 1: Morphological analysis

Submechanism	***Design ideas***				
Handshell	3D printed	milling	injection molding	ceramic	glass
Fingers	solid model	finger joints			
Closing joint	rod mechanism	pulleys	lever mechanism	rack and pinion	gears
Transmission muscle power	shoulder strap				
Transmission motor power	planetary gear	pinion gear	worm gear mechanism		
Decoupling motor power	clutch	sensor	asymetric		
Blocking (incl. deblocking)	single ratchet	force sensor	enclosed by shape	worm wheel	
Cabel tension	clock spring	coil spring	motor		
Opening hand	force sensor	button			

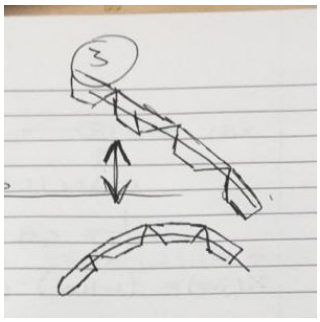

Figure A.1: Fingers - finger joints

Figure A.2: Closing joint - lever mechanism

Figure A.3: Closing joint - gears

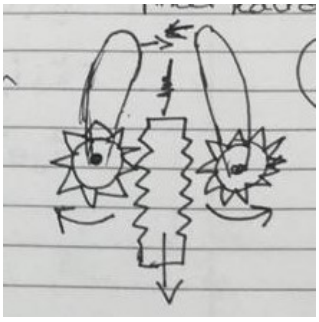

Figure A.4: Closing joint - rack and pinion

B SolidWorks model

Appendix B presents an overview of the SolidWorks model (figure B.1) and the SolidWorks exploded view drawings of three assemblies: the hybrid hand (figure B.5), the motor mechanism (figure B.7) and the linkage mechanism (figure B.6). The appendix also contains several figures for clarification. Figure B.2 shows the differences between the old and new design for the inner shell. Figure B.3 shows how the motor axis is attached to the worm axis. Figure B.4 shows the design of the ball receiver to which the cable and simulator are attached.

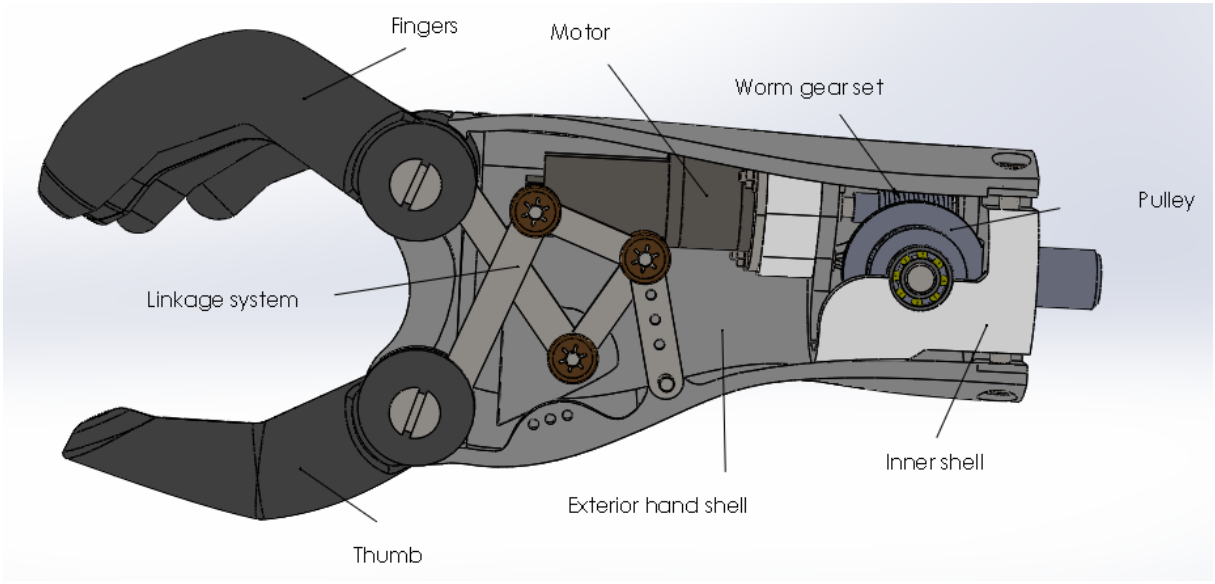

Figure B.1: SolidWorks overview

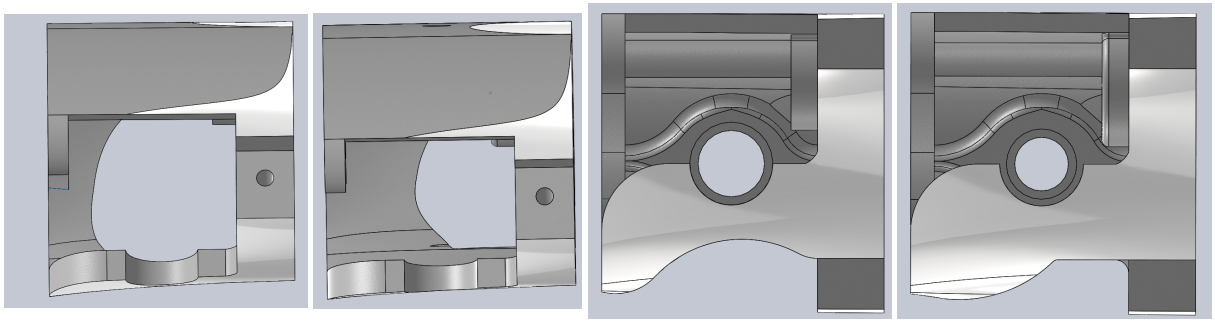

(a) Riho, bottom view (b) New, bottom view (c) Riho, side view (d) New, side view

Figure B.2: Inner shell

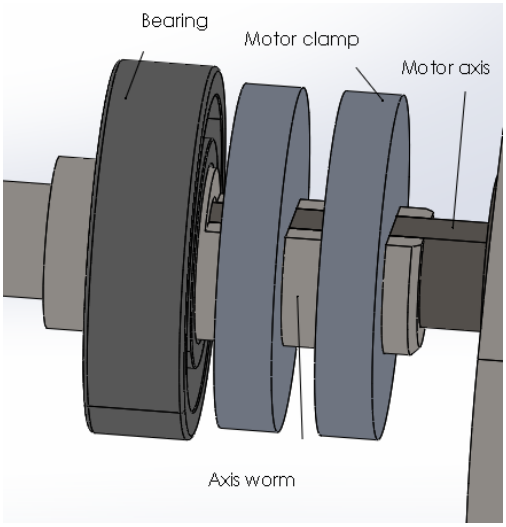

Figure B.3: Mounting motor axis

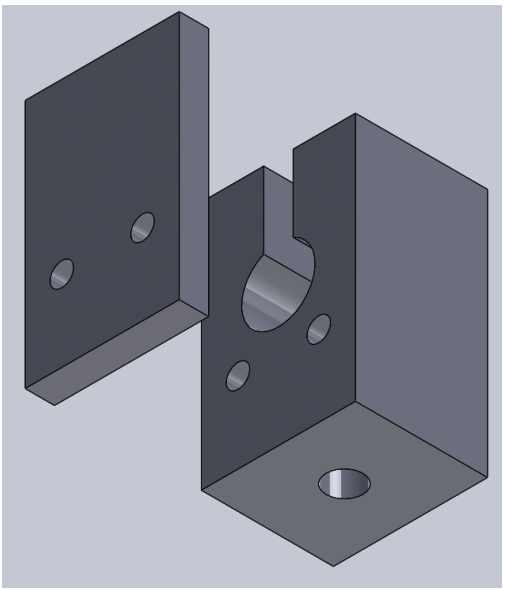

Figure B.4: Ball receiver

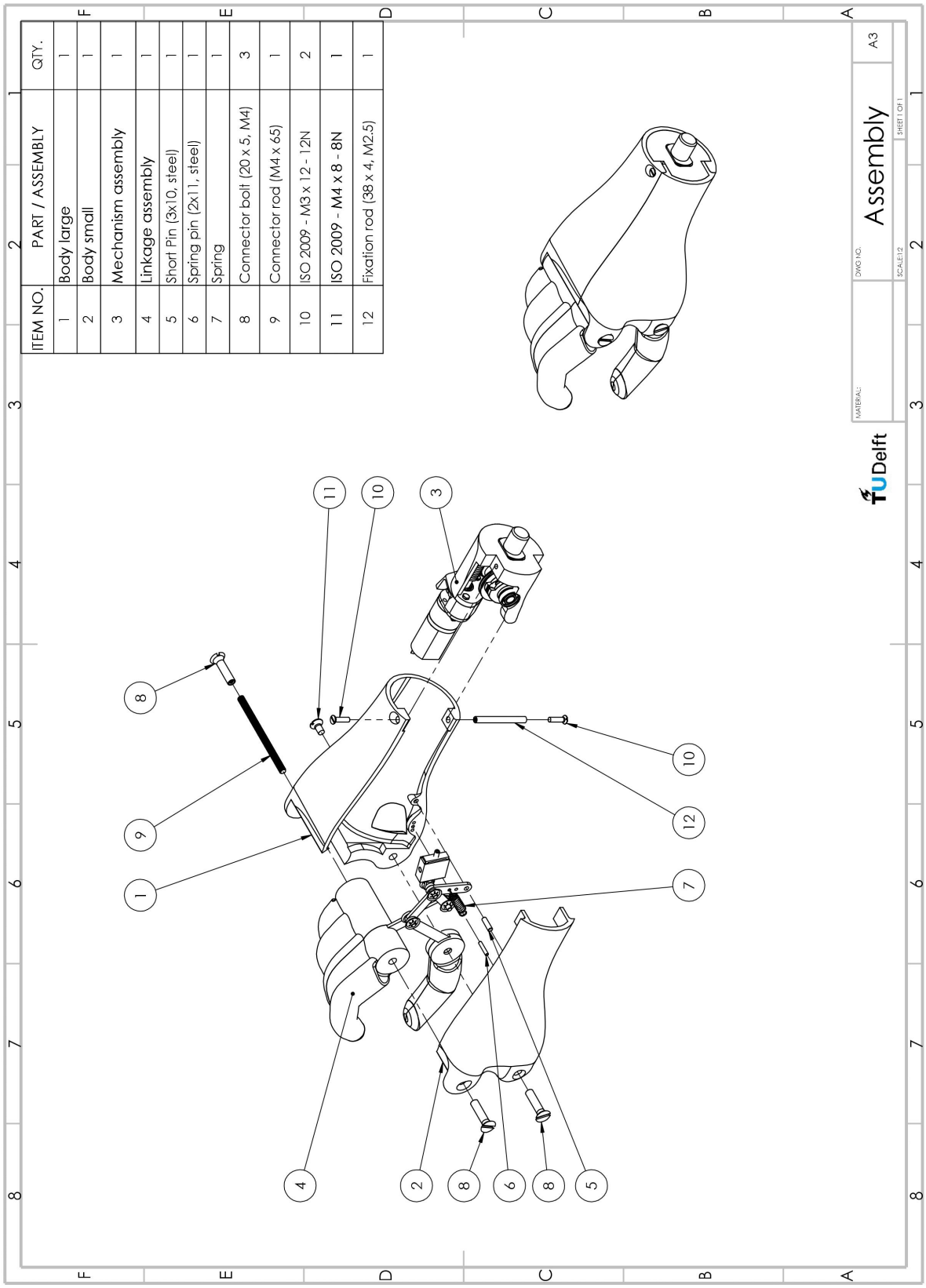

Figure B.5: Exploded view hybrid hand

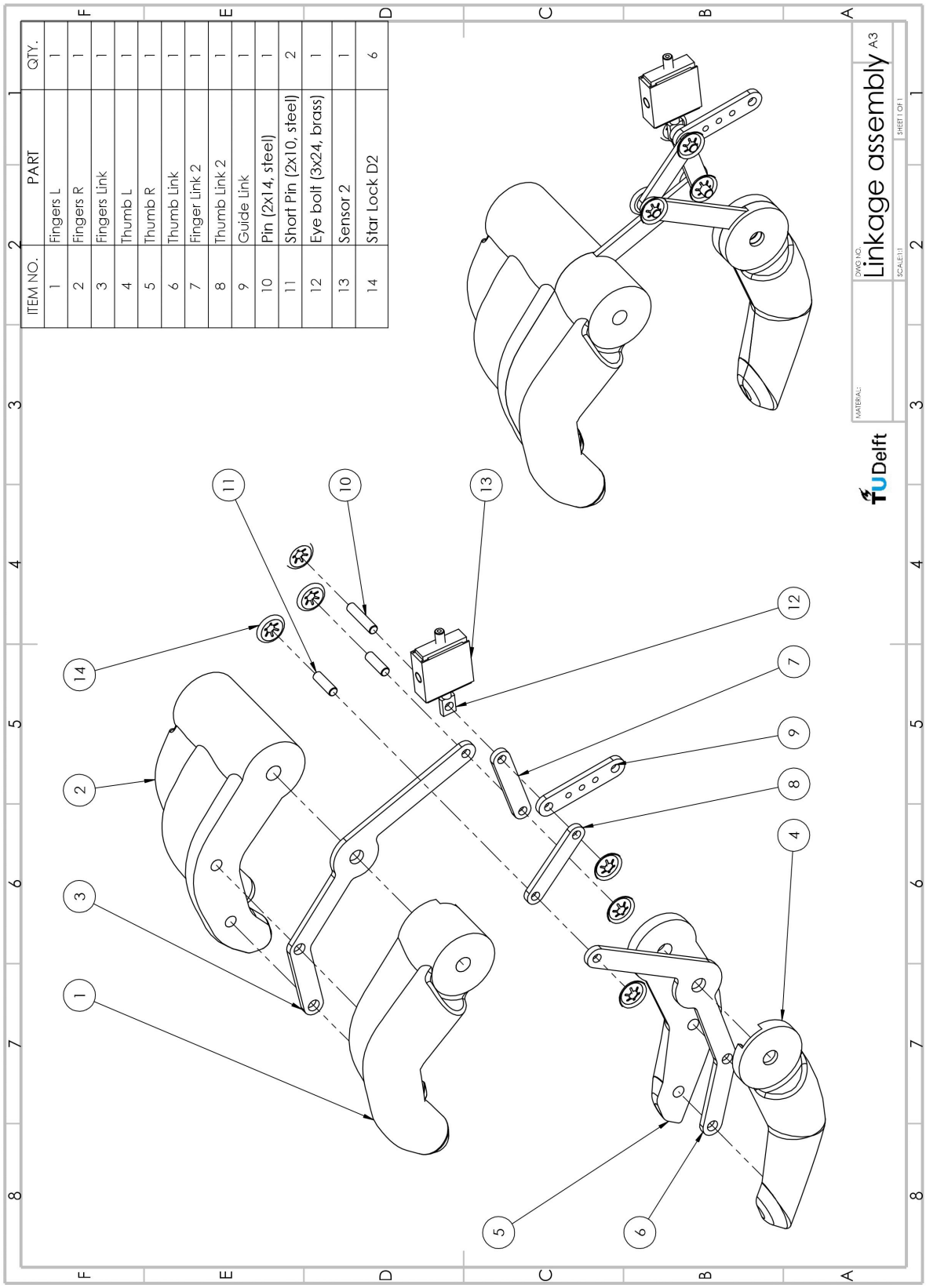

Figure B.6: Exploded view linkage mechanism assembly

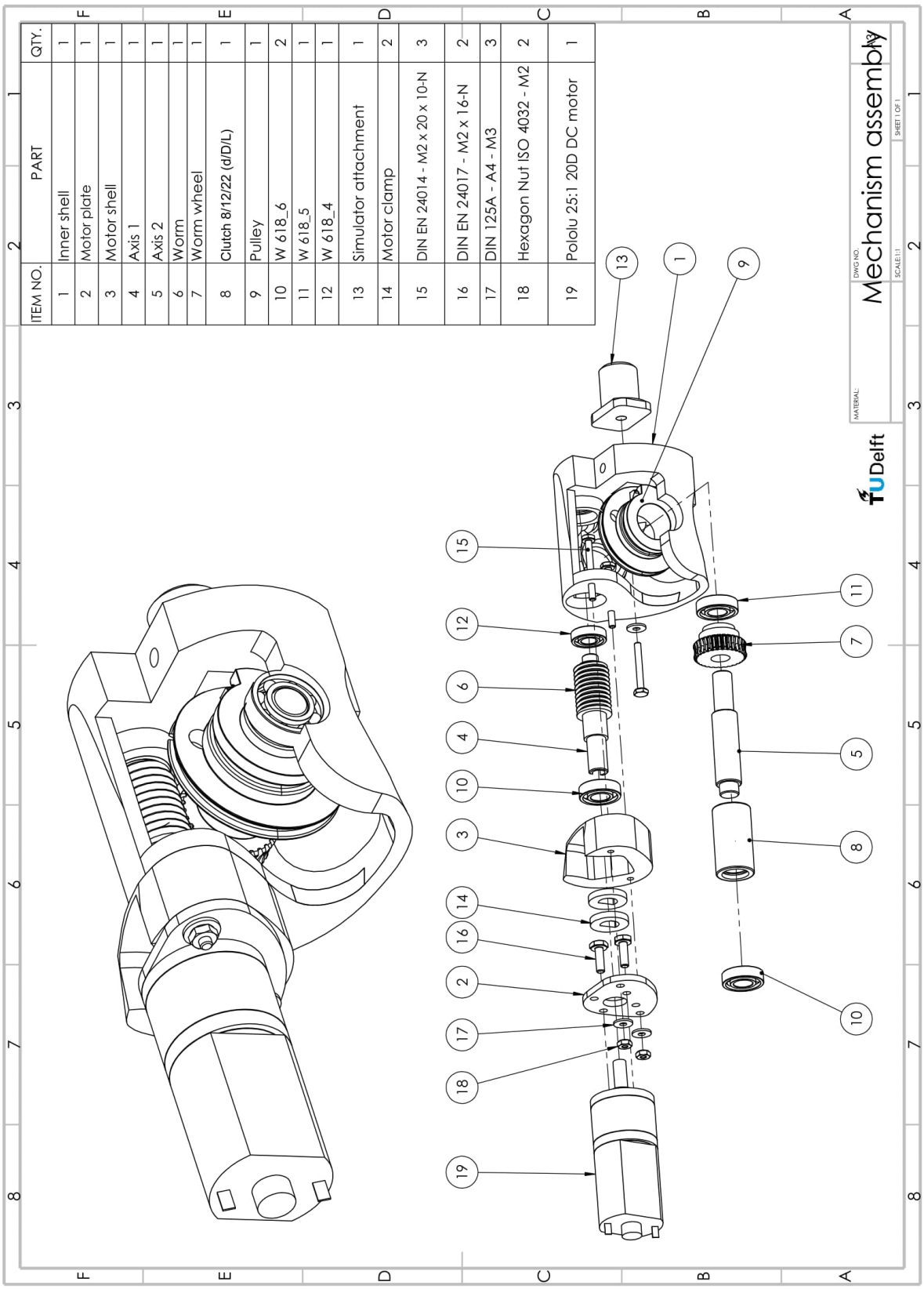

Figure B.7: Exploded view motor mechanism assembly

C Component list

This appendix contains an overview of all components used in the hybrid hand, see table 2.

Table 2: Component list

Part	*Specification*	*Product origin*	*QTY.*
Body large		3D printed	1
Body small		3D printed	1
Short pin	3x10, steel	TU Delft	1
Spring pin	2x11, steel	TU Delft	1
Spring		TU Delft	1
Connector bolt	20 x 5, M4	TU Delft	3
Connector rod	M4 x 65	TU Delft	1
Countersunk screw	ISO 2009 - M3 x 12 - 12N	TU Delft	2
Countersunk screw	ISO 2009 - M4 x 8 - 8N	TU Delft	1
Fixation rod	38 x 4, M2.5	TU Delft	1
Fingers L		3D printed	1
Fingers R		3D printed	1
Fingers Link 1		Laser cut	1
Thumb L		3D printed	1
Thumb R		3D printed	1
Thumb Link 1		Laser cut	1
Finger link 2		Laser cut	1
Thumb Link 2		Laser cut	1
Guide link		Laser cut	1
Pin	2x14, steel	TU Delft	1
Short Pin	2x10, steel	TU Delft	2
Eye bolt	Modelcraft 10258/AS-M3, brass	Ordered: Conrad	3
Force sensor	Futek	TU Delft	2
Starlock	Diameter 2 mm	TU Delft	6
Inner shell		3D printed	1
Motor plate		Laser cut	1
Motor shell		3D printed	1
Axis 1		IWM	1
Axis 2		IWM	1
Worm	Reely worm gear set, module 0,75 brass/steel 20	Ordered: Conrad	1
Worm wheel	Reely worm gear set, module 0,75 brass/steel 20	Ordered: Conrad	1
Clutch	Reely 8/12/22 (d/D/L)	Ordered: Conrad	1
Pulley		3D printed	1
Ball bearing	W 618_6	Ordered: SKF	2
Ball bearing	W 618_5	Ordered: SKF	1
Ball bearing	W 618_4	Ordered: SKF	1
Simulator attachment		IWM	1
Motor clamp		Laser cut	2
Hexagon bolt	DIN EN 24014 - M2 x 20 x 10-N	TU Delft	3
Hexagon bolt	DIN EN 24017 - M2 x 16-N	TU Delft	2
Plain washer	DIN 125A - A4 - M3	TU Delft	3
Hexagon nut	ISO 4032 - M2	TU Delft	2
Motor	25:1 Metal Gearmotor 20Dx41L mm 6V	Ordered: Open Circuit	1
Steel wire	1 meter	TU Delft	1
Arduino Nano	Joy-it V3 Development-board ATMega328	Ordered: Conrad	1
Motor driver	Motor driver - DUAL TB6612FNG (1A)	Ordered: Antatrek	1
Voltage regulator	Linear LM350T 1.2 V 3 A TO-220-3	Ordered: Conrad	1
Amplifier	INA125P Texas Instruments	Ordered: RS-online	2
Hand glove		TU Delft	1

D Ball receiver

This appendix shows an example of a ball receiver. This design could be ordered or used as an example to remake for a future design of the hybrid hand.

Figure D.1: Ball receiver to order as improvement [1]

E Complete hybrid hand

This appendix shows three figures of the complete hybrid hand.

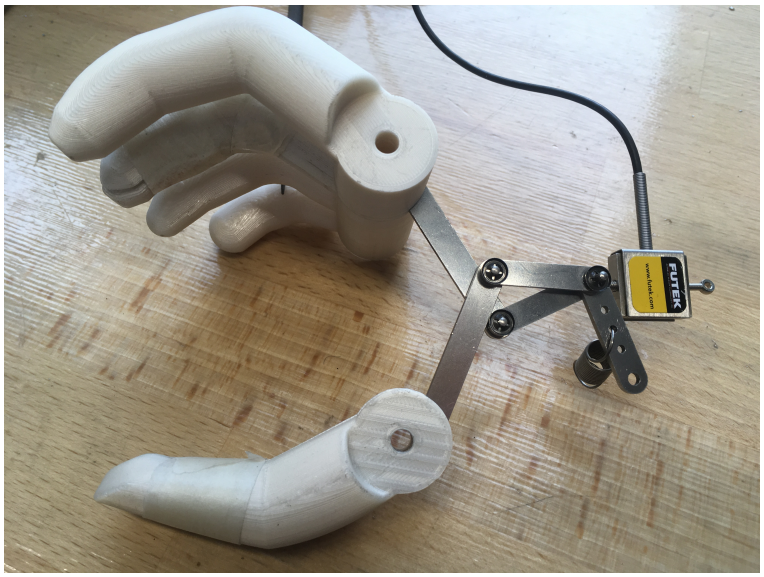

Figure E.1: Linkage mechanism

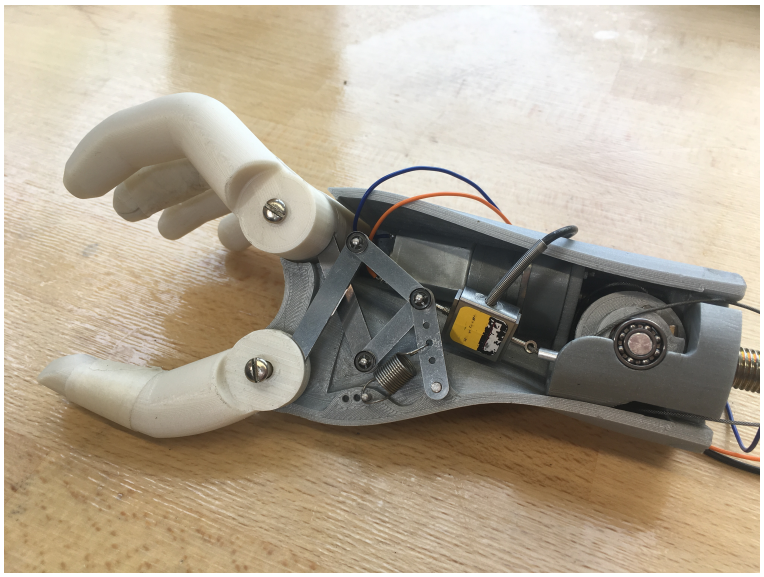

Figure E.2: Hybrid hand without small body

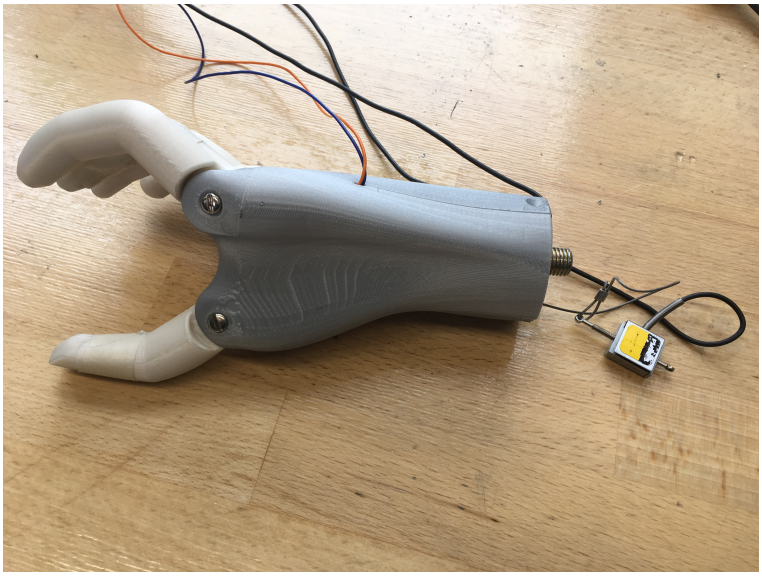

Figure E.3: Hybrid hand with small body